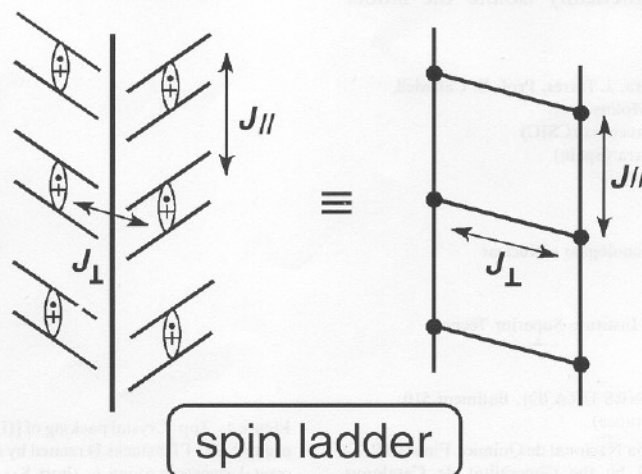


Electrocristal-
 lization of the
 donor D and the
 $n\text{Bu}_4\text{N}$ salt of the acceptor A gave
 crystals (structure in the center) whose
 donor stacks form a two-leg spin ladder

223 K by localization of unpaired elec-
 trons in D_2^+ units (principles of
 the construction depicted at the

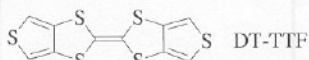
bottom). For fur-
 ther details, see
 the following
 pages.



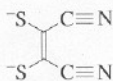
An Organic Spin-Ladder Molecular Material**

Concepció Rovira,* Jaume Veciana, Elisabet Ribera, Judit Tarrés, Enric Canadell, Roger Rousseau, Montserrat Mas, Elies Molins, Manuel Almeida, Rui T. Henriques, Jorge Morgado, Jean-Philippe Schoeffel, and Jean-Paul Pouget

Materials with a ladder type arrangement of the spins ("spin-ladder compounds") have brought a lot of excitement to the quantum magnets community.^[1] The initial expectations concerning these materials have been fully confirmed by recent findings of a puzzling dependence of the bulk magnetic properties with the even/odd number of legs in the ladder. Recent results on metal-based compounds (mainly oxides) indicate that while odd-leg ladders are gapless and have magnetic behavior similar to one-dimensional chains, even-leg ladders have only short-range order and a finite spin gap. In addition, holes injected into even-leg ladders are predicted to pair and possibly show superconductivity.^[2] Until now only very few two-leg and three-leg ladder compounds formed by connected chains of transition metal atoms have been studied.^[2a, 3] Because of their structural flexibility molecular solids offer many possibilities to finely tune interesting physical situations such as those exhibited by spin-ladder materials. Molecular organic solids with this kind of behavior could be obtained by assembling a finite number of molecular chains one next to the other to form "ladder-structures" of increasing width. We have succeeded in preparing and characterizing [(DT-TTF)₂][Au(mnt)₂] (**1**, DT-TTF = "dithiophentetrathiafulvalene",



DT-TTF



mnt

mnt = maleonitrile dithiolate), one of these wide spin-ladder organic solids.

By analogy with the metallic α phases of the (Per)₂M(mnt)₂ family (Per = perylene, M = metal), which crystallize in a structure containing pairs of perylene chains surrounded by M(mnt)₂ chains,^[4] we sought to construct a ladder molecular organic compound by replacing perylene by an appropriate aromatic donor. As electron donor we chose DT-TTF,^[5] which tends to stack to form chainlike structures and which contains sulfur atoms on the periphery that are able to promote close contacts between the chains,^[6] to provide the rungs of the spin ladder system. As counterion we chose the closed-shell monoanion [Au(mnt)₂]⁻,^[7] which might magnetically isolate the ladder chains.

As counterion we chose the closed-shell monoanion [Au(mnt)₂]⁻,^[7] which might magnetically isolate the ladder chains.

[*] Dr. C. Rovira, Prof. J. Veciana, E. Ribera, J. Tarrés, Prof. E. Canadell, Dr. R. Rousseau, Dr. M. Mas, Dr. E. Molins
Institut de Ciència dels Materials de Barcelona (CSIC)
Campus de la U. A. B., E-08193 Bellaterra (Spain)
Fax: Int. code +(3)580-5729
e-mail: c.rovira@icmab.es

Dr. M. Almeida
Departamento de Química, Instituto Tecnológico e Nuclear
P-2686 Sacavém Codex (Portugal)

Dr. R. T. Henriques, Dr. J. Morgado
Departamento de Engenharia Química, Instituto Superior Técnico
P-1096 Lisboa Codex (Portugal)

Prof. J.-P. Pouget, J.-P. Schoeffel
Laboratoire de Physique des Solides (CNRS URA 02), Batiment 510
Université Paris-Sud, F-91405 Orsay (France)

[**] This work was supported by the Programa Nacional de Química Fina (CIRIT-CICYT; grant, QFN93-4510-C01) and by the Generalitat de Catalunya (SGR95-0057) in Barcelona, by PRAXIS 2/2.1/QUI/203/94, in Sacavém and by JNICT-CSIC agreement. E. R. thanks CIRIT for a fellowship.

The target compound [(DT-TTF)₂][Au(mnt)₂] (**1**) was obtained as dark needles by electrocrystallization from a dichloromethane solution containing the donor and the tetrabutylammonium salt of [Au(mnt)₂]⁻. The mixed valence character of this salt was confirmed by the presence in the near infrared (NIR) spectrum of the characteristic "A" band of the mixed valence states centered at 2700 nm.^[8] Compound **1** crystallizes in the monoclinic system,^[9] and the asymmetric unit comprises one molecule of DT-TTF and 0.5 molecule of [Au(mnt)₂]. At room temperature the DT-TTF and [Au(mnt)₂] molecules form segregated regular stacks of donors and acceptors along *b* in a herringbone pattern (Figure 1). Inside each stack, donors **D** (DT-TTF) and acceptors **A** ([Au(mnt)₂]) slip parallel to the shortest axis of the molecule and have interplanar distances of 3.555(3) and 3.581(4) Å, respectively. The DT-TTF stacks are arranged in pairs related by a twofold screw axis, and they alternate with single stacks of [Au(mnt)₂] along the *a*-*c* direction. Apparently the pairs of organic donor stacks form a structural two-leg ladder, since they are strongly linked by three interstack S···S close contacts (Figure 1b). As shown later, the double donor stacks form a two-leg spin ladder below 225 K due

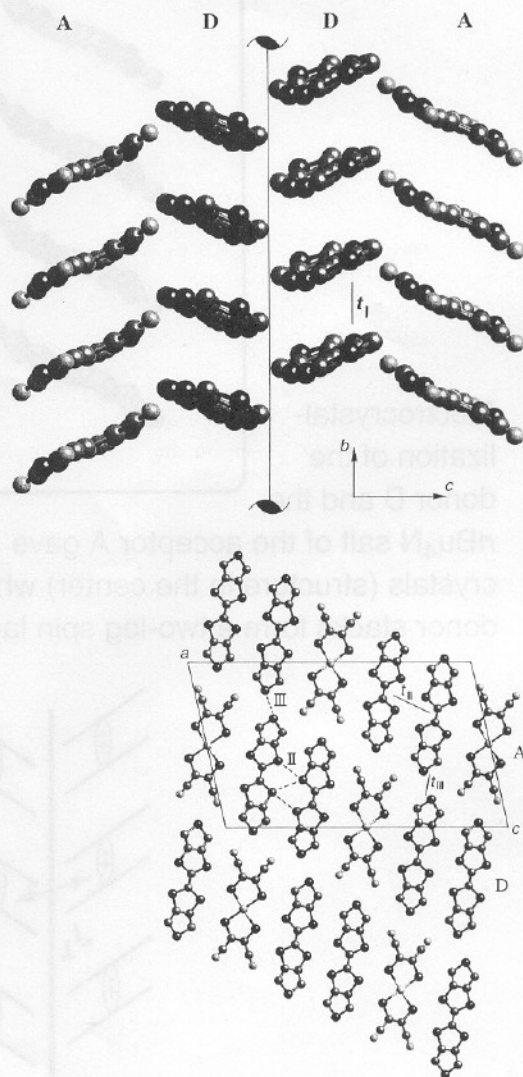


Figure 1. Top: Crystal packing of [(DT-TTF)₂][Au(mnt)₂] (**1**) at 293 K showing the organic DT-TTF stacks **D** related by a twofold screw axis. Bottom: Projection of the crystal structure along *b*, short S···S contacts (between 3.460 and 3.944 Å) are indicated by dotted lines. This figure represents the average structure. It does not include the local dimerization discussed in the text.

to the localization of unpaired electrons in $(\text{DT-TTF})_2^+$ dimeric units.

The electrical conductivity along the chain axis b is thermally activated and is about 8 S cm^{-1} at room temperature. Its temperature dependence (Figure 2) has an inflexion point at about 220 K, denoting that the gap increases significantly below this temperature. The thermopower $S(T)$ is positive (about $40 \mu\text{V K}^{-1}$ at 300 K), indicating a hole transport as expected in a partially oxidized (quarter empty) donor band.

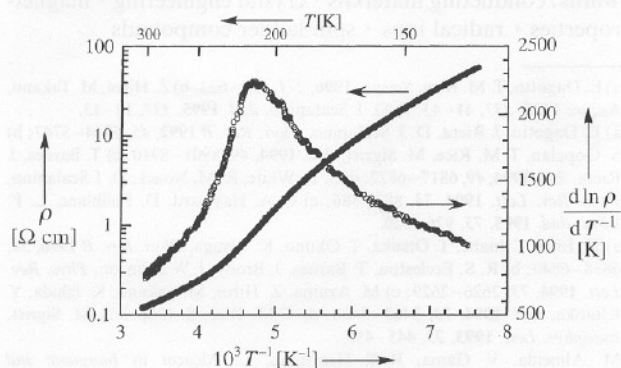


Figure 2. Electrical resistivity ρ of $(\text{DT-TTF})_2[\text{Au}(\text{mnt})_2]$ as a function of the reciprocal temperature (left) and its first derivative, $d \ln \rho / d T^{-1}$ (right), measured along the needle axis b by the standard four-probe method.

Taken together, the 2:1 stoichiometry, the closed-shell character of $[\text{Au}(\text{mnt})_2]^-$, and the electrical transport measurements clearly show that below 220 K the unpaired electrons are quite localized in the organic, DT-TTF, interacting double chains. Consequently, depending on the strength of the interactions within and between the double chains, this organic system could well fulfill the requirements for spin-ladder behavior. In order to quantify this point we have calculated the HOMO–HOMO transfer integrals for the different donor···donor interactions of the lattice.^[110] There are only three types of DT-TTF interactions (Figure 1): 1) those within the DT-TTF molecular chains (I), 2) those connecting the two molecular chains that form the pair (II), and 3) those between the extremities of the molecules in different paired chains (III). The calculated $t_{\text{HOMO-HOMO}}$ transfer integrals are 36 meV for t_1 , 21 meV for t_{II} , and 6 meV for t_{III} . Three important implications may be drawn from these values. First, the transfer integral t_{III} between the pairs of chains is quite small relative to those within chains (t_1 and t_{II}). Thus, the different pairs of chains of the lattice are probably quite isolated. Second, the transfer integrals up the chain (t_1) and coupling the two paired chains (t_{II}) are nonnegligible. Third, these transfer integrals within chains (t_1 and t_{II}), although nonnegligible, are smaller than those of related molecular metals. This agrees with the relatively high but activated conductivity. These three observations suggested a possible spin-ladder behavior for **1** in which the paired chains constitute the ladder. However, before pursuing along this line, we must consider additional structural features that explain more clearly the observed electronic localization.

In order to study this point, X-ray diffuse scattering experiments were performed.^[111] X-ray patterns taken at 15 K reveal a weak scattering consisting of single diffuse lines located midway between successive layers of main Bragg reflections perpendicular to the chain direction b . Its reduced wave vector ($0.5b^*$) shows that a dimerization is achieved in the chain direction. These lines are broader than the experimental resolution, which means that the dimerization takes place only on a local scale. At 15 K their half width at half maximum (HWHM) along b is of

$\Delta Q = 0.035 \text{ \AA}^{-1}$. The inverse of this quantity, corrected by the (gaussian) resolution, leads to an intrachain correlation length ξ_b of 60(40) \AA , if one assumes an intrinsic Lorentzian (gaussian) profile for the diffuse scattering. As shown in Figure 3 (top) these diffuse lines begin to broaden substantially above about 225 K and at 295 K ξ_b amounts to about 20 \AA .

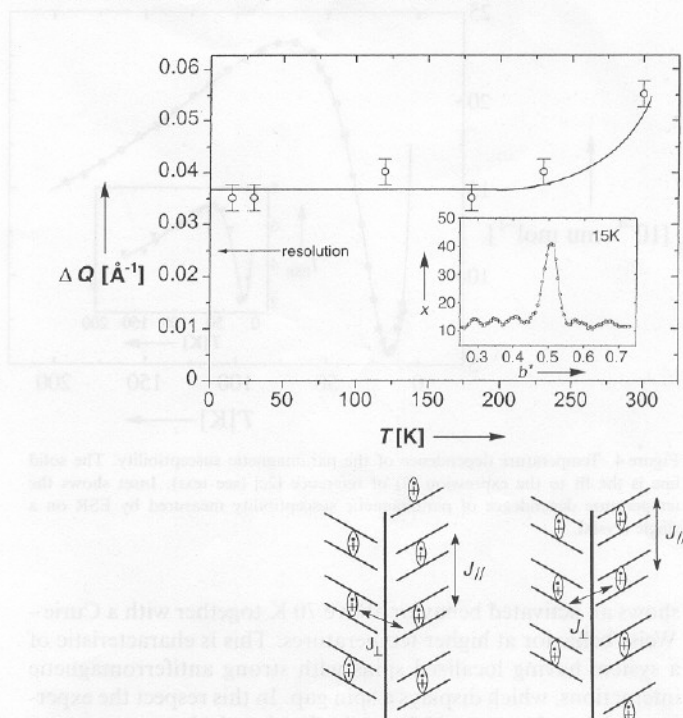


Figure 3. Top: Thermal dependence of the HWHM along the b axis of the $1/2b^*$ diffuse lines of **1**. The inset shows the profile along b^* of such a line (x is the number of counts in arbitrary units). Bottom: Schematic illustration of the two possible two-leg ladders formed by the dimerization of DT-TTF stacks, where J_{\parallel} is the exchange coupling along the chains, and J_{\perp} is the coupling along the rungs.

The weakness of the scattering suggests that the dimerization occurs on the pairs of strongly linked DT-TTF stacks. The observation of diffuse lines means that there is no sizable phase relation between the dimerization of first pairs of adjacent stacks. Their finite width shows that the dimerization locally breaks the twofold screw axis symmetry, which relates the two stacks that form the ladder. As there are two ways to break this symmetry (see Figure 3, bottom), it can be easily understood that their simultaneous realization on a given pair of stacks will limit the intrachain correlation length. From the previous determination of ξ_b , one can estimate an average domain size at low temperature of about $L_b (= \pi \xi_b) = 150 \text{ \AA}$ (i.e. $40b$). Therefore, this structural study indicates that at low temperature (15–225 K) this molecular system consists of isolated ladders with a finite number (about 40) of rungs. The decrease of this number above 225 K leads to a better conducting state.

In this picture each dimer has one localized electron (Figure 3, bottom). Since $[\text{Au}(\text{mnt})_2]^-$ has a closed-shell nature, the magnetic properties of this compound arise only from the spins located in the organic $(\text{DT-TTF})_2^+$ units of the ladders, in agreement with the observed ESR g factor. Thus the ESR g factor of the radical cation $[\text{DT-TTF}]^+$ in solution,^[15] is very close to the average g value of the crystals of **1**. As expected, the minimum g value is observed when the magnetic field is applied parallel to the stacking b axis.^[12] The relatively large paramagnetism thus associated with these $(\text{DT-TTF})_2^+$ units does not show any significant anomaly around 220 K, where the trans-

port properties displayed anomalies; this fact indicates that, due to electronic correlations, the spin and charge degrees of freedom in the DT-TTF chains are separated. The most important result (Figure 4) is that the static magnetic susceptibility^[13] $\chi(T)$

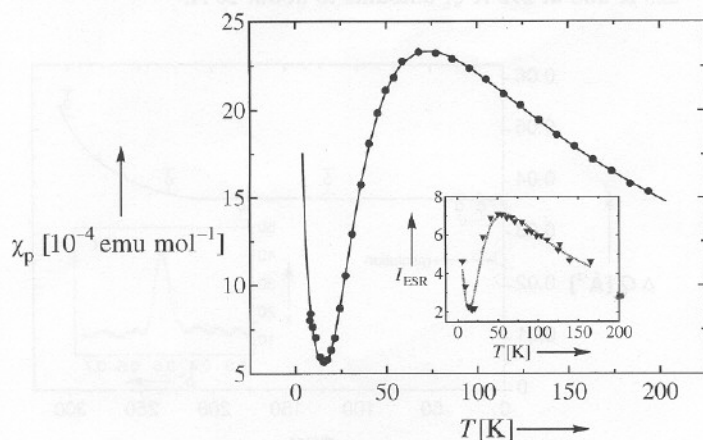


Figure 4. Temperature dependence of the paramagnetic susceptibility. The solid line is the fit to the expression (2) of reference [2c] (see text). Inset shows the temperature dependence of paramagnetic susceptibility measured by ESR on a single crystal.

shows an activated behavior above 70 K together with a Curie–Weiss behavior at higher temperatures. This is characteristic of a system having localized spins with strong antiferromagnetic interactions, which displays a spin gap. In this respect the experimental data from 8 to 45 K can be fitted to the low temperature expression for the susceptibility of a two-leg ladder model found by Troyer et al. [Eq. (1)],^[14] where α is a constant corresponding

$$\chi_{\text{ladder}} = \alpha T^{-1/2} \exp(-\Delta/kT) \quad (1)$$

to the dispersion of the excitation energy, and Δ is the finite energy gap in the spin-excitation spectrum. For such a fit Equation (2), which takes into account the Curie contribution due

$$\chi = f\chi_{\text{ladder}} + (1-f)\chi_{\text{Curie}} \quad (2)$$

both to the finite sizes of the ladders and to the magnetic defects present in the crystals, was used. In Equation (2) f is the molar fraction of [(DT-TTF)₂]⁺ units forming the regular ladder. The resulting parameters of this fit were $f = 0.98$, $\alpha = 7.22 \times 10^{-4} \text{ emu K}^{1/2} \text{ mol}^{-1}$, and $\Delta/k = 78 \text{ K}$ ($r^2 = 0.9972$). The experimental susceptibility was also fitted with the expression (2) given by Barnes and Riera,^[2c] for a two-leg ladder model (solid line in Figure 4), which provides the exchange coupling parameters J_{\parallel} and J_{\perp} , of the ladder spin configuration. The resulting parameters of such a fit were $f = 0.980$, $J_{\parallel}/k = -83 \text{ K}$ and $J_{\perp}/k = -142 \text{ K}$ ($r^2 = 0.9989$). The ratio between J_{\parallel} and J_{\perp} is in good agreement with the ratio between the transfer integrals evaluated from the t_t and t_{\parallel} values once the dimeric nature of the elementary building block of the ladder is taken into account. The spin gap has also been calculated from the resulting values of J_{\parallel} and J_{\perp} by using the expression $\Delta = |J_{\perp}| - |J_{\parallel}| + J_{\parallel}^2/2J_{\perp}$,^[14] to give $\Delta/k = 83 \text{ K}$, in good agreement with the previous value. The intensity of the ESR signal, which is proportional to the paramagnetic spin susceptibility, also exhibits the same thermal dependence as the static spin susceptibility (inset of Figure 4), confirming that the spin-ladder behavior occurs on the organic [(DT-TTF)₂]⁺ stacks.

The results presented here characterize [(DT-TTF)₂][Au(mnt)₂] as the first example of a purely organic system with a ladder spin configuration that shows this magnetic behavior below 225 K. This result opens new possibilities to apply supramolecular chemistry for tailoring ladder architectures with different structural characteristics and promising magnetic properties.

Received: April 17, 1997 [Z 103601E]
German version: *Angew. Chem.* 1997, 109, 2417–2421

Keywords: conducting materials · crystal engineering · magnetic properties · radical ions · spin-ladder compounds

- [1] a) E. Dagotto, T. M. Rice, *Science* 1996, 271, 618–623; b) Z. Hiroi, M. Takano, *Nature* 1995, 337, 41–43; c) D. J. Scalapino, *ibid.* 1995, 337, 12–13.
- [2] a) E. Dagotto, J. Riera, D. J. Scalapino, *Phys. Rev. B* 1992, 45, 5744–5747; b) S. Gopalan, T. M. Rice, M. Sigrist, *ibid.* 1994, 49, 8901–8910; c) T. Barnes, J. Riera, *ibid.* 1994, 49, 6817–6822; d) S. R. White, R. M. Noack, D. J. Scalapino, *Phys. Rev. Lett.* 1994, 73, 882–886; e) C. A. Hayward, D. Poilblanc, L. P. Lévy, *ibid.* 1995, 75, 926–929.
- [3] a) H. Imai, T. Inabe, T. Otsuka, T. Okuno, K. Awaga, *Phys. Rev. B* 1996, 54, 6838–6840; b) R. S. Eccleston, T. Barnes, J. Brody, J. W. Johnson, *Phys. Rev. Lett.* 1994, 73, 2626–2629; c) M. Azuma, Z. Hiroi, M. Takano, K. Ishida, Y. Kitaoka, *ibid.* 1994, 73, 3463–3466; d) T. M. Rice, S. Gopalan, M. Sigrist, *Europhys. Lett.* 1993, 23, 445–450.
- [4] M. Almeida, V. Gama, R. T. Henriques, L. Alcácer in *Inorganic and Organometallic Polymers with Special Properties*; (Ed.: R. M. Laine), Kluwer, Dordrecht, The Netherlands, 1992, pp. 163–177.
- [5] C. Rovira, J. Veciana, N. Santaló, J. Tarrés, J. Cirujeda, E. Molins, J. Llorca, E. Espinosa, *J. Org. Chem.* 1994, 59, 3307–3313.
- [6] J. J. Novoa, M. C. Rovira, C. Rovira, J. Veciana, J. Tarrés, *Adv. Mater.* 1995, 7, 233–237.
- [7] A. Davison, N. Edelstein, R. H. Holm, A. H. Maki, *Inorg. Chem.* 1963, 2, 1227–1232.
- [8] J. B. Torrance, B. A. Scott, B. Welber, F. B. Kaufmann, P. E. Seiden, *Phys. Rev. B* 1979, 19, 730–741.
- [9] Crystallographic data for C₂₈H₁₆N₄S₁₆Au: crystal dimensions 0.37 × 0.23 × 0.065 mm; $M_r = 1110.31$, monoclinic, space group $P2_1/n$, $a = 16.334(1)$, $b = 3.912(1)$, $c = 27.348(2) \text{ \AA}$, $\beta = 101.787(6)^\circ$; $Z = 2$; $V = 1710.7(2) \text{ \AA}^3$, $\rho_{\text{calc}} = 2.16 \text{ g cm}^{-3}$. Data were collected at 293 K on an Enraf-Nonius CAD4 diffractometer equipped with a Mo X-ray tube, and a graphite monochromator selected Mo κ_{α} radiation (absorption coefficient $\mu = 5.31 \text{ mm}^{-1}$). Data collection up to $2\theta = 62^\circ$ and $-23 \leq h \leq 23$, $0 \leq k \leq 5$, $-39 \leq l \leq 0$ affords 7898 reflections measured with $\omega - 2\theta$ scans. Lorentz, polarization, and absorption (DI-FABS: max/min absorption factors 1.254/0.793) effects were corrected. The structure was refined using full-matrix least-squares methods (SHELXL-93). The minimized function was $\omega(F_o^2 - F_c^2)^2$ with $\omega = 1/\sigma^2 F^2 + (AP)^2 + BP$ and $A = 0.0419$, $B = 0.57$, $P = [Max(F_o) + 2F_c]/3$ and s , the standard deviation estimated from counting statistics. At convergence the final R indices were $R_1 = 0.068$, $wR_2 = 0.078$ (for all data) and $R_1 = 0.027$, $wR_2 = 0.066$ (for $I > 2\sigma(I)$ reflections). The final max/min residuals were 1.11/−0.91 e \AA^{-3} . Crystallographic data (excluding structure factors) for the structure reported in this paper have been deposited with the Cambridge Crystallographic Data Centre as supplementary publication no. CCDC-100375. Copies of the data can be obtained free of charge on application to The Director, CCDC, 12 Union Road, Cambridge CB2 1EZ, UK (fax: int. code +(1223)336-033; e-mail: deposit@chemcrs.cam.ac.uk).
- [10] As in previous studies of related materials (L. F. Veiros, M. J. Calhorda, E. Canadell, *Inorg. Chem.* 1994, 33, 4290–4294), the calculations use an extended Hückel type hamiltonian (R. Hoffmann, *J. Chem. Phys.* 1963, 39, 1397–1412) and a modified Wolfsberg–Helmholz formula (J. H. Ammeter, H.-B. Bürgi, J. Thibault, R. Hoffmann, *J. Am. Chem. Soc.* 1978, 100, 3686–3692) to calculate the nondiagonal H_{ij} matrix elements and a single- ζ atomic orbital basis set.
- [11] The experiment was performed with the so-called “fixed film-fixed crystal” method with a monochromatized Cu κ_{α} ($\lambda = 1.542 \text{ \AA}$) beam.
- [12] The ESR spectra consists in a single Lorentzian line in all the orientations of the crystal with respect to the external magnetic field. The room temperature line-widths measured in the three orthogonal orientations of the crystal are $\Delta H_{pp} = 42, 25$, and 26 G , with g factors of 2.0127, 2.0050, and 2.0020, respectively.
- [13] Magnetic susceptibility was measured by the Faraday method in the range 4–300 K in a polycrystalline sample with an applied magnetic field of 1 T. A correction for the diamagnetic contribution estimated as $4.6 \times 10^{-4} \text{ emu mol}^{-1}$ from tabulated Pascal constants was applied.
- [14] M. Troyer, H. Tsunetsugu, D. Würtz, *Phys. Rev. B* 1994, 50, 13515–13527.